processes

MDPI

Article

Recovery of Ammonium from Biomass-Drying Condensate Via Ion Exchange and Its Valorization as a Fertilizer

Jianzhi Song [1], Jari Heinonen [2] and Tuomo Sainio [3,*]

[1] School of Engineering Science, LUT University, Sammonkatu 12, 50130 Mikkeli, Finland
[2] UPM-Kymmene Oyj, Kaukaankatu 23, 53200 Lappeenranta, Finland
[3] School of Engineering Science, LUT University, Mukkulankatu 19, 15210 Lahti, Finland
* Correspondence: tuomo.sainio@lut.fi

Abstract: In this study, an industrial biomass-drying wastewater condensate containing > 3200 mg/L NH_4^+ and >8900 mg/L CH_3COO^- was treated in ion-exchange columns for the recovery of NH_4^+. Two commercial resins (CS12GC and CS16GC) were studied on laboratory and pilot scales. CS16GC outperformed CS12GC by achieving better separation at the condensate temperature (60 °C), which was energy-efficient regarding NH_4^+ removal. K_3PO_4 was used for regeneration to produce a liquid compound fertilizer containing nutrient elements (N, K, and P) as a byproduct. The N/K ratio in the byproduct was found to be adjustable by varying the operating parameters. Regeneration with 2 mol/L K_3PO_4 gave a higher regeneration efficiency (97.67% at 3 BV and ~100% at 4 BV). The stability tests performed on a laboratory scale showed that the cyclic runs of the column separation process were steady and repeatable. Based on the outcomes of the laboratory-scale tests, the pilot-scale tests applied a loading volume of 7 BV. The pilot column purified the feed and achieved the target NH_4^+ level in the treated effluent within the seven tested cycles, revealing that the industrial application of the cation ion-exchange resin CS16GC is worth further study.

Keywords: ammonium acetate; ion-exchange column; pilot scale; industrial condensate; fertilizer byproduct

Citation: Song, J.; Heinonen, J.; Sainio, T. Recovery of Ammonium from Biomass-Drying Condensate Via Ion Exchange and Its Valorization as a Fertilizer. *Processes* **2023**, *11*, 815. https://doi.org/10.3390/pr11030815

Academic Editor: Monika Wawrzkiewicz

Received: 31 January 2023
Revised: 1 March 2023
Accepted: 7 March 2023
Published: 9 March 2023

1. Introduction

In this study, commercial ion-exchange resins were applied to recover ammonium from an industrial waste stream containing excess ammonium. The industrial wastewater studied was a condensate coming out of a condenser after a drying procedure in a thermal treatment process of municipal sewage sludge developed by Endev Ltd. (Helsinki, Finland). The condensate contained concentrated ammonium acetate (>3200 mg/L, or 179.2 mmol/L NH_4^+), which must be pretreated before being fed into a municipal wastewater treatment plant. Additionally, the organic anion content (>8900 mg/L, or 151.5 mmol/L CH_3COO^-) differentiates this waste stream from typical ammonium wastewater. This work reveals the feasibility of the ion-exchange process in the presence of plentiful acetate ions.

Ammonium is well known as one of the major nutrients essential for fertilizers used for agricultural purposes, as well as a pollutant discharged into natural water bodies through various sources, such as municipal wastewater, landfill leachate, and agricultural runoff [1]. The removal of ammonium has been carried out using several processes, which can be categorized as biological, chemical, and physicochemical processes.

Biological processes employ naturally existing microorganisms to biologically degrade ammonium through nitrification and denitrification in bioreactors. The conventional biological process does not operate well with shock loads of ammonia or high ammonium concentrations (>3200 mg/L NH_4^+ in this case) [2,3]. Chemical processes include chemical precipitation and chemical or catalytic/photocatalytic oxidation. Physicochemical processes comprise membrane filtration, air stripping, adsorption, and ion exchange [4–8]. Struvite

precipitation has been reported to be inhibited by high acetate concentrations but not low acetate concentrations (<100 mg/L) [9,10]. It has been reported that ammonium phosphomolybdate works as a cation exchanger to remove dyes from water [11,12]. The Keggin structure is a possible option to precipitate ammonium. Bernardi et al. (2012) studied catalytic wet air oxidation regarding ammonium acetate aqueous solutions [2]. Ammonium oxidation was successful, but a high temperature and pressure (at 200 °C under 50 bar air) and platinum-based catalysts were required, making oxidation a complicated and expensive alternative.

Ion exchange is a conventional and well-developed technique, while numerous ion exchangers and applications have yet to be further conceived and studied [13]. To deal with ammonium, ion-exchange processes can generate a purified eluent and enrich ammonium to recover ammonium for further usage, e.g., fertilizer. In the scenario of industrial wastewater with a high ammonium content, a large volume of ion exchangers packed in a column is expected, and thus, commercial resins are favorable choices that are supplied with a vast availability and have a high dynamic capacity and good stability.

In the current work, conventional commercial ion exchangers were used to recover ammonium from industrial wastewater. Both laboratory- and pilot-scale column studies were carried out, aiming for industrial application. CS12GC and CS16GC, strong-acid cation-exchange (SAC) resins (gel-type sulfonated polystyrene-divinylbenzene beads), were studied. Such SAC resins are versatile separation materials that are sometimes overlooked. Besides water softening, their ion-exchange property can be used, for example, to liberate organic acids from their salts [14], and their electrolyte exclusion property can be used to separate strong electrolytes from weak electrolytes and neutral species [15]. The hydrophobic nature of their polymer matrix can be utilized in the adsorption of harmful organic compounds [16]. When choosing ion exchangers, the most important factor to consider is stability (chemically and mechanically) on a scale of years or even decades of industrial operation, on which polymeric resin is a reliable option. Although the cost of an ion exchanger no longer matters concerning the designed operating lifespan, it is worth noting that commercial resins are relatively low-cost and standard products. In this study, the commercial resins were used in the potassium form to recover ammonium in a way that resulted in a byproduct that could be used a nutrient-ratio-adjustable compound fertilizer.

2. Materials and Methods

2.1. Chemicals

Potassium chloride (KCl), potassium hydroxide (KOH), orthophosphoric acid (H_3PO_4), potassium phosphate tribasic monohydrate ($K_3PO_4 \cdot H_2O$), ammonium chloride (NH_4Cl), and ammonium acetate (CH_3COONH_4/NH_4Ac) were supplied by VWR Chemicals and used without further purification in the preparation of experimental solutions. All chemicals were of reagent grade. Purified water was used in all experiments and in the preparation of all solutions.

Two commercial cation-exchange resins from Finex Oy (Kotka, Finland) were used: CS12GC, with a 6.0 wt.% cross-linking degree and a particle diameter of 0.38 mm, and CS16GC, with an 8.0 wt.% cross-linking degree and a particle diameter of 0.36 mm. The original resins were in the H^+ form, and they were converted to the K^+ and NH_4^+ forms using KOH and NH_4Cl solutions, respectively.

Authentic condensate water originated from an industrial sludge combustion facility (Rovaniemi, Finland), in which the process was designed and developed by Endev Ltd. (Finland). The sample was analyzed for the concentration of cations and anions. The composition of the condensate is listed in Table 1. The pH of the condensate water sample was 5.42.

Table 1. Composition of the condensate water samples.

Content	Concentration (mg/L)
NH_4^+	3226
Na^+	44
K^+	24
Ca^{2+}	25
CH_3COO^-	8939
SO_4^{2-}	78
PO_4^{3-}	4

Artificial condensate water was prepared using purified water and NH_4Ac with a targeting concentration of 0.179 mol/L. The ammonium recovery experiments regarding the condensate were all based on the artificial condensate water. The pH of the artificial condensate water was about 7. It was used in the experiments without pH adjustments.

2.2. Ammonium Recovery Experiments

2.2.1. Laboratory-Scale Experiments

Laboratory-scale experiments were conducted with a chromatographic column with an inner diameter of 15 mm and a resin bed height of 20 cm (V_{bed} = 35.34 mL). A downward flow was applied at certain flow rates. The temperatures studied were room temperature and condensate temperature (60 °C).

Loading tests with the artificial condensate water were conducted for both resins (CS12GC and CS16GC) in the K^+ form. The flow rate (Q) was 3 BV/h (1.767 mL/min), and the volume of condensate fed to the column (V^F) was 20–22 BV. The temperature of the column was set to room temperature, as well as 60 °C, for both resins. The regeneration of CS16GC in the NH_4^+ form was studied at 60 °C with 1 mol/L and 2 mol/L K_3PO_4 solutions. The resin was prepared using 1 mol/L NH_4Cl and washed with an adequate amount of water. Regeneration was carried out with a Q of 2 BV/h (1.178 mL/min) and a V^F of 5 BV.

Cyclic runs with the condensate were performed at 60 °C for 7 cycles with the CS16GC resin in the K^+ form as the starting separation material, using 0.179 mol/L NH_4Ac and 2 mol/L K_3PO_4 solutions. The cyclic steps were run at the same flow rate (Q) of 4 BV/h (2.356 mL/min): (1) the loading of the resin with the artificial condensate water (V^F = 12 BV); (2) washing with water to remove excess condensate water from the resin bed (V^F = 4 BV); (3) the regeneration of the resin with 2 mol/L K_3PO_4 (V^F = 3 BV); and (4) washing with water to remove excess K_3PO_4 from the resin bed (V^F = 4 BV).

2.2.2. Pilot-Scale Experiments

Pilot-scale experiments were implemented in a chromatographic column with an inner diameter of 140 mm with a downward flow at 60 °C. The resin used was CS16GC, and the bed height was 42.5 cm (V_{bed} = 6.54 L). The regeneration agent (2 mol/L K_3PO_4) was prepared by mixing the KOH and H_3PO_4 solutions with the desired concentrations. A total of 7 cycles were conducted at a flow rate of 4 BV/h, and sampling was carried out regularly. Table 2 below shows the feed volumes united in BV during the cyclic steps.

Table 2. Feed volumes (V^F in BV) used in the pilot-scale ammonium removal experiments.

Cycle	1	2	3	4	5	6	7
Loading	7.0	7.0	7.0	7.0	7.0	7.0	7.0
Water washing	2.0	2.0	2.0	2.0	2.0	2.0	2.0
Regeneration	3.0	3.0	4.0	4.0	3.0	3.0	3.0
Water washing	4.0	4.0	4.0	4.0	4.0	4.0	4.0

2.3. Chemical Analyses

Samples were selected on the basis of online detector signals and taken for offline analyses for the quantification of ammonium and potassium. The ammonium, potassium, acetate, and phosphate ion contents in the samples were analyzed using Ion Chromatography (IC, Thermo Fisher ICS-1100). The anions were analyzed according to the standard SFS-EN ISO 10304-2 with a column of IonPac (AG22 − 4 × 50 mm + AS22 − 4 × 250 mm) and eluent (4.5 mM Na_2CO_3 + 1.4 mM $NaHCO_3$). Cations were analyzed according to the standard SFS-EN ISO 14,911 with a column of IonPac (CG12A − 4 × 50 mm + CS12A − 4 × 250 mm) and eluent (22 mN H_2SO_4).

2.4. Modeling and Simulation

The recovery of ammonium from an acetate-rich solution in an ion-exchange column packed with a strong-acid cation-exchange resin was simulated by solving mass balance equations numerically. The mass balance for a differential volume element in the column was written as

$$\frac{\partial c_j}{\partial t} + \frac{1-\varepsilon_{\text{bed}}}{\varepsilon_{\text{bed}}}\frac{\partial \overline{q}_j}{\partial t} + u^{\text{L}}\frac{\partial c_j}{\partial z} = D_{\text{ax},j}\frac{\partial^2 c_j}{\partial z^2} \tag{1}$$

where t (s) and z (m) are the time and position coordinates, respectively; c is the liquid-phase molar concentration (mol/L); $\overline{q}$ is the volume-average solid-phase concentration (mol/L); u^{L} is the interstitial flow velocity (m/s); ε is the porosity of the bed (0.40); and D_{ax} is the axial dispersion coefficient (m^2/s).

The intraparticle diffusion of the ions was calculated by using the linear driving force approximation, which resulted in

$$\frac{\partial \overline{q}_j}{\partial t} = \frac{60 D_{\text{s},j}}{d_{\text{p}}^2}\left(\hat{q}_j - \overline{q}_j\right) \tag{2}$$

where the equilibrium concentration of the ammonium cations in the resin, $\hat{q}$, was calculated from

$$\hat{q}_{NH_4{}^+} = Q_{\text{IX}}\frac{K_{\text{NH}_4/\text{K}}c_{\text{NH}_4^+}}{c_{K^+} + K_{\text{NH}_4/\text{K}}c_{\text{NH}_4^+}} \tag{3}$$

and that of the potassium cations from the charge balance was calculated from

$$\hat{q}_{K^+} = Q_{\text{IX}} - c_{\text{NH}_4^+} \tag{4}$$

In the equilibrium functions, Q_{IX} is the total ion-exchange capacity of the resin (mol/L) in the swollen state.

The selectivity coefficient $K_{\text{NH}_4/\text{K}}$ = 0.88 was taken from the literature [17,18], and it was regarded as being independent from temperature. The same selectivity coefficient value was used for both resins because of their chemical similarity.

The axial dispersion coefficient was calculated from

$$D_{\text{ax}} = \frac{H_{\text{col}}u^{\text{L}}}{N_{\text{Pe}}} \tag{5}$$

where H_{col} is the height of the column (m), and the dimensionless Peclet number, N_{Pe}, was calculated by using the correlation of Chung and Wen [19]:

$$N_{\text{Pe}} = \frac{H_{\text{col}}}{\varepsilon_{\text{bed}}d_{\text{p}}}\left(0.2 + 0.11N_{\text{Re}}^{0.48}\right) \tag{6}$$

$$N_{\text{Re}} = \frac{\rho u^{\text{L}}\varepsilon_{\text{bed}}d_{\text{p}}}{\eta} \tag{7}$$

where ρ and η are the density and viscosity of the solvent (water), respectively.

The PDE system was solved using the method of lines. The first derivatives in the spatial coordinates were approximated using the five-point biased upwind scheme, and the second derivatives were approximated using a five-point central scheme [20]. The resulting ODE system, together with Equation (3), was integrated with a modernized version of VODE [21]. Danckwerts boundary conditions were used at the column inlet and outlet. The intraparticle diffusion coefficients and the total ion-exchange capacity were estimated based on experimental breakthrough curves.

3. Results and Discussion

3.1. The Determination of Temperature and Resin Cross-Linking Degree

The commercial cation-exchange resins CS12GC and CS16GC were both prepared in the K^+ form and studied for the recovery of ammonium from ammonium acetate-containing water that was prepared to represent a biomass-drying condensate (Table 1). The condensate that comes out of the condenser is about 60 °C according to the process design. Loading (i.e., feeding into the resin bed) was therefore studied at 22 °C and 60 °C.

As shown in Figure 1a,b, K^+ ions were displaced from the resin, and NH_4^+ ions were taken up by the resin [22]. The breakthrough curves are qualitatively similar for both resins and at both temperatures, but there are important differences. The breakthrough curves are steeper for CS12GC than for CS16GC at both 22 °C (Figure 1a) and 60 °C (Figure 1b). However, the mid-point of the breakthrough curves for CS12GC (green symbols) is eluted earlier than for CS16GC (red symbols). The feed level of the NH_4^+ concentration was reached after approximately 16 BV feeding for CS12GC and approximately 19 BV for CS16GC. These observations suggest that mass transfer is faster with CS12GC, whereas CS16GC has a higher ion-exchange capacity.

These conclusions are corroborated by the simulation results. The experimental data were correlated by fitting ion-exchange capacity Q_{IX} and intraparticle diffusion coefficient D_s into the experimental breakthrough profiles. The best-fit values are given in Table 3, and the simulated breakthrough curves are shown as solid lines in Figure 1a,b.

Table 3. Values of the parameters in Equations (1)–(7) estimated from experimental breakthrough curves.

Parameter	CS12GC	CS16GC
$K_{NH_4/K}$	0.88	0.88
Q_{IX} (mol/L)	3.35	3.70
D_s (m^2/s) at 20 °C	1.0×10^{-11}	0.4×10^{-11}
D_s (m^2/s) at 60 °C	2.1×10^{-11}	0.9×10^{-11}

The volumetric ion-exchange capacity of CS16GC was found to be approximately 10% higher than that of CS12GC. This is because the higher degree of cross-linking in CS16GC reduces the swelling of the resin in an aqueous environment, and the mole amount of functional groups per unit volume of the column is higher. The difference in cross-linking is also reflected in the diffusion coefficients. They were approximately 60% lower in the more densely cross-linked CS16GC because the denser medium increases the diffusion path length and increases the friction of hydrated ions.

No effect of temperature on ion-exchange capacity or NH_4/K selectivity was observed when correlating the data, and the same values of Q_{IX} and $K_{NH_4/K}$ were used at both temperatures. This was expected because the standard enthalpy of ion-exchange reactions for simple 1:1 systems is quite small, typically about $\pm(0.1 - 0.5)$ kJ/eq [23,24]. The effect of temperature on the diffusion rates was found to be very similar in both resins; D_s more than doubled when the temperature increased from 20 °C to 60 °C.

To achieve a certain emission standard for ammonium, CS16GC can deal with more condensate wastewater than CS12GC (Figure 1c,d). The difference is more obvious for CS16GC, while NH_4^+ ions first appeared in the samples collected from the outlet of the column after feeding about 5 BV at room temperature but 7 BV at 60 °C (Figure 1c).

Regarding the volume-average capacity, the integration of the elution profile of NH_4^+ ions gives the cumulative amount in the effluent. At a certain feeding volume, for instance, 6 BV, CS16GC can remove more NH_4^+ ions at 60 °C than at room temperature. Whilst at a pre-set breakthrough point, to achieve a desired NH_4^+ concentration in the eluent, CS16GC can treat a larger volume of condensate at 60 °C (Figure 1d).

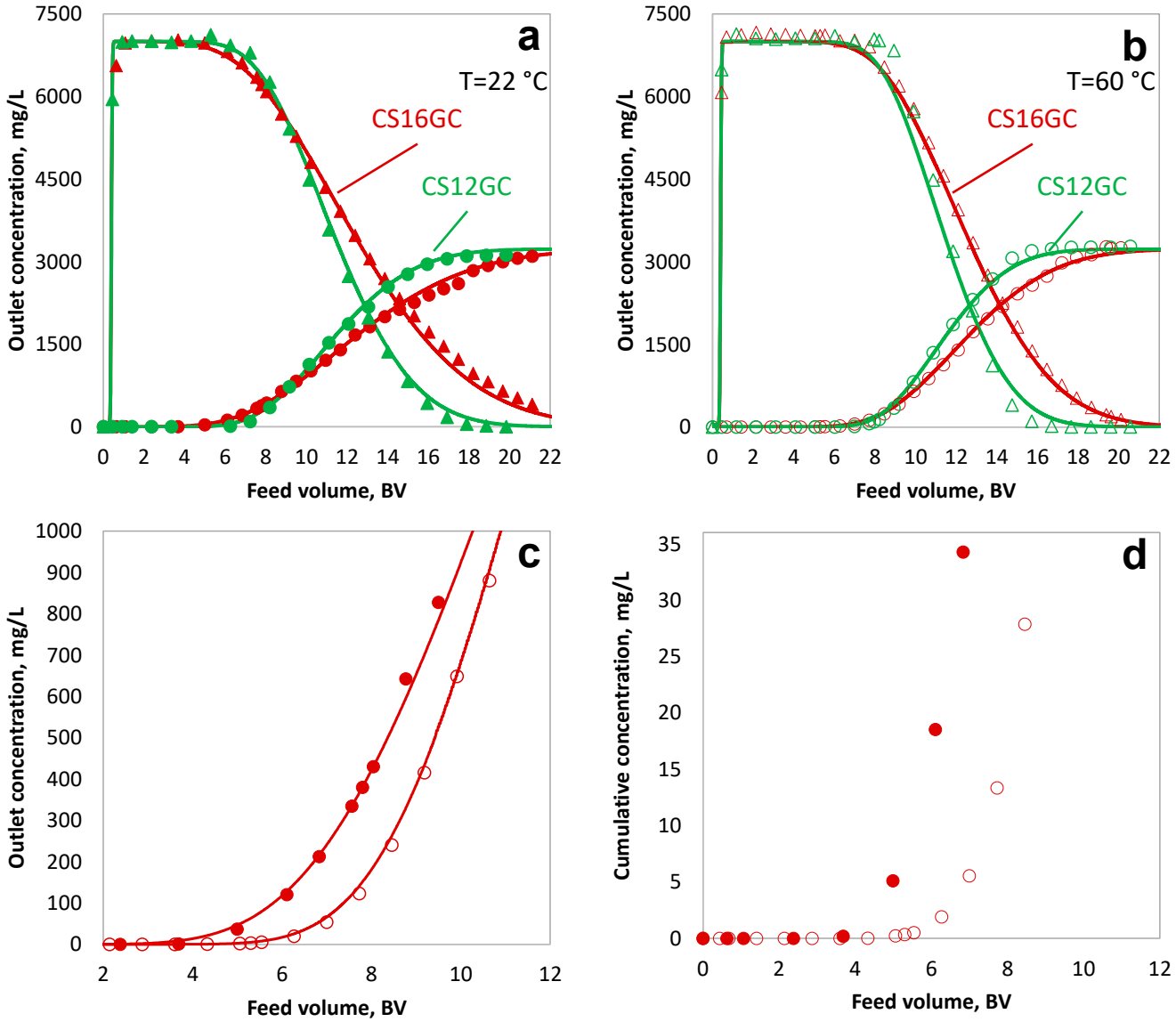

Figure 1. Ammonium and potassium profiles at the column outlets for the removal of ammonium from condensate with CS12GC and CS16GC cation-exchange resins in K^+ form of (**a**) temperature at 22 °C, (**b**) temperature at 60 °C; (**c**) ammonium concentrations at the column (CS16GC) outlet; (**d**) cumulative ammonium concentrations (CS16GC column). Experimental (symbols) and simulated (lines) data for the loading step (V_{bed} = 35.34 mL, Q = 3 BV/h, feed 0.179 mol/L NH_4Ac). Open symbols: T = 60 °C, filled symbols: T = 22 °C. Red symbols and lines: CS16GC resin; green symbols and lines: CS12GC resin. Triangles: K^+; circles: NH_4^+.

A higher temperature led to a more flexible polymer network and a higher thermal energy in the resin, which both support better diffusion, resulting in deeper breakthrough curves (better separation). This is consistent with the former observations of Yoon et al. [25]. Additionally, from the energy efficiency of the condensate treatment process point of view, it is not necessary to cool down or heat up the condensate stream coming from the drying

process if the ion-exchange recovery can be carried out at an elevated temperature. Thus, 60 °C is the better temperature to apply to ammonium recovery from condensate.

The experimental data showed that the operating exchange capacities of CS16GC reached 63.20 g NH_4^+/L at 60 °C and that those of CS12GC reached 53.35 g NH_4^+/L at 60 °C (Figure S1). Theoretically, CS16GC, which has a higher cross-linking degree, contains less water (or more polymer) per unit volume and, thus, should have a higher unit volume uptake towards ammonium, which is consistent with the experimental result. Based on the comparison of the effect of temperature and the resin cross-linking degree, CS16GC and 60 °C were chosen for ammonium recovery tests with an ion-exchange column.

Table 4 shows a comparison between several studied strong-acid cation-exchange resins, which were operated in column processes for the removal of ammonium from an aqueous phase. CS16GC in the current study showed the highest unit-bed volume cation (NH_4^+) exchange capacity among the listed resins. Similarly, the study of Gefeniene et al. (2006) showed that Purolite C160 MBH exhibited a high capacity for treating an influent with a concentrated ammonium content (>3200 mg/L NH_4^+) [26]. CS16GC exhibited an operating capacity of 55.86 g NH_4^+/L at 60 °C at breakthrough, corresponding to 50% of the initial concentration, while the operating capacity of Purolite C160 MBH was 37.08 g NH_4^+/L.

Table 4. Comparison of operating capacities towards NH_4^+ of different strong-acid cation-exchange resins in column processes.

Resin	C_0 (mg/L)	T (°C)	Q (BV/h)	q_m (g/L)	Reference
CS16GC	3312.1	60	3.0	63.20	Current study
				55.86 *	Current study
CS12GC	3197.7	60	3.0	53.35	Current study
				49.42 *	Current study
Purolite C160 MBH	3744.0	20	2.7	37.08 *	[26]
Amberjet 1500H	600.9	20	5.0	35.46	[27]
Lewatit S 100	600.9	20	5.0	31.68	[27]
Amberlite 252H	600.9	20	5.0	29.52	[27]
KU-2-8	51.4	20	40.9	34.95	[28]
Amberlyst 15WET	51.4	22	6.0	4.57	[29]
Purolite C100E	17.4	30	1.9	7.66	[30]

C_0: influent NH_4^+ concentration (mg/L); T: temperature; Q: flow rate; q_m: maximum operating NH_4^+ exchange capacity. * Operating capacity at breakthrough corresponding to 50% of the initial concentration.

The acetate concentration at the outlet of the ion-exchange column during the loading test with CS16GC in the K^+ form at 60 °C is shown in Figure S2. It can be suggested that the acetate ions eluted out steadily. The pH profile of the loading test using CS16GC at 60 °C is shown in Figure S3. It follows the acetate profile and levels off at about 7, corresponding to the pH of the feed. Considering the performance of the resins towards the recovery of NH_4^+, as shown in Figure 1, the presence of acetate in the feed does not prevent the use of the cation ion-exchange resin.

Potassium acetate (KAc) is the main form of the ions in the effluent from the loading step. In its pure form, KAc is an additive (named E261) used for food preservation [31]. Moreover, it is one of the deicers used to melt snow and ice on the road in cold weather, where purity is not emphasized [32]. Although the ion-exchange process was designed to act as a pre-treatment before the feed to municipal wastewater treatment, the direct utilization of a KAc-containing solution might be another option, while further studies of the economic and environmental impacts are demanded.

3.2. Regeneration Efficiency

The regeneration of the spent resin was studied with CS16GC at 60 °C because that combination was found to be the best for ammonium recovery. The regeneration agents used were 1 mol/L and 2 mol/L K_3PO_4 solutions. The idea was to generate a useful byprod-

uct that contains N, P, and K elements. The pH values of these regeneration agents were 13 and 13.6, respectively. According to the phosphate speciation curves, the dominant anion species was PO_4^{3-} with a small portion of HPO_4^{2-} [33]. In fact, the strong-acid cation resin with the 8% cross-linking degree (CS16GC in this case) had a greater preference for NH_4^+ than Na^+ and H^+. According to references [17,18,24], the rational thermodynamic equilibrium constants are $\kappa_{K^+}^{NH_4^+} = 0.88$, $\kappa_{Na^+}^{NH_4^+} = 1.29$, and $\kappa_{H^+}^{NH_4^+} = 2.01$ for sulfonated polystyrene cation-exchange resins with an 8% cross-linking degree. Though the ion-exchange capacity of the resin remains the same, the capacity towards NH_4^+ at the breakthrough point is affected by the equilibrium constant. Accordingly, H^+- and Na^+-form resins would hold a narrower exchange front and, thus, more processing volume and a higher breakthrough capacity than K^+-form resin [28]. However, using the resin in the H^+ form requires a concentrated acid (such as HCl) for regeneration, which causes corrosion problems, especially in metallic pump parts, and it results in acidic waste streams that are hard to treat or utilize. By contrast, using the Na^+ form leads to less valuable fertilizer byproducts containing a high amount of Na but barely any K elements.

The elution of NH_4^+ came out of the column earlier and faster with the 2 mol/L K_3PO_4 solution than with the 1 mol/L solution (Figure 2a). The concentration of NH_4^+ at the outlet of the column remained at a level of >5000 mg/L until the feeding of 3 BVs of 1 mol/L K_3PO_4 and 2 BVs of 2 mol/L K_3PO_4. The regeneration efficiency reached 93.20% and 97.67% when the regeneration was conducted for 3 BVs with 1 mol/L and 2 mol/L K_3PO_4, respectively (Figure 2b). Since the regeneration efficiency of the 4 BV feeding of 2 mol/L K_3PO_4 would increase to almost 100% but with the cost of 33.33% more agent volume, for regeneration, it was considered reasonable to apply 2 mol/L K_3PO_4 and 97.67% efficiency at 3 BV feeding in the cyclic runs that followed.

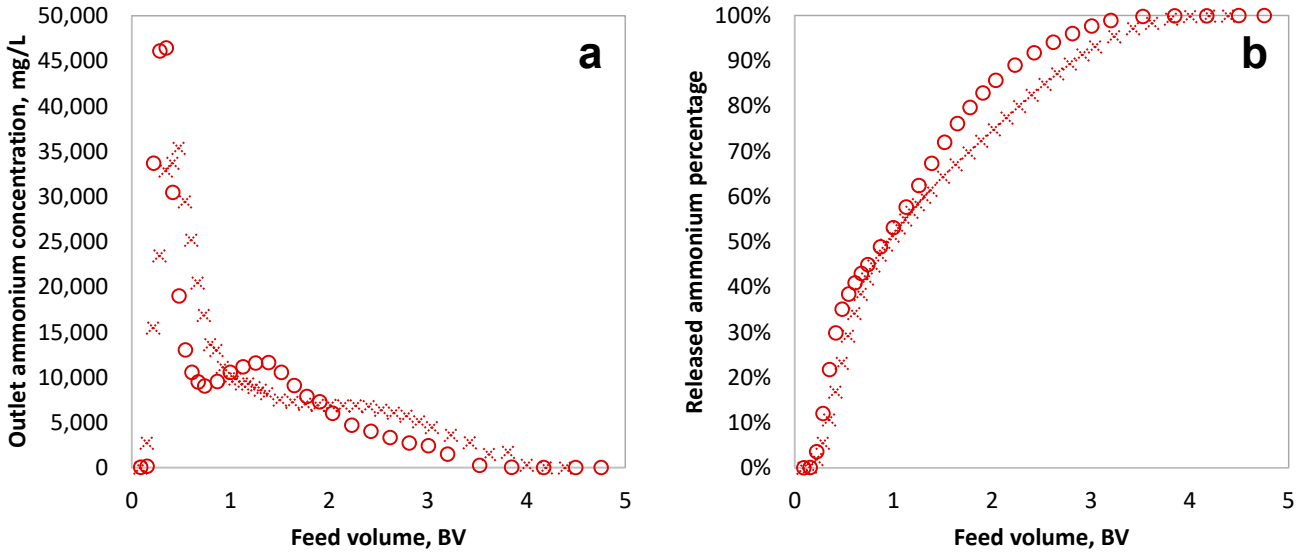

Figure 2. (**a**) Ammonium concentrations during the regeneration of CS16GC resin with K_3PO_4, (**b**) the regeneration efficiency. (V_{bed} = 35.34 mL, Q = 2 BV/h, at 60 °C, resin was pre-saturated with 1 mol/L NH_4Cl). Dash-line crosses: 1 mol/L K_3PO_4; solid-line circles: 2 mol/L K_3PO_4.

The fluctuation in the regeneration profiles is possibly caused by dispersion in the column. There is a density difference between the regeneration agent and the liquid, which is already inside the column before regeneration starts. The floating force of the low-density solution and the pumping flow cause mixing in the bed. The same situation applies to the cyclic runs on laboratory and pilot scales.

3.3. Stability of the Separation Process

The stability of the separation process was tested on the laboratory scale in the sequence of loading, washing, regeneration, and second washing repeatedly over seven cycles in total. As shown in Figure 3, where data are shown for cycles 1, 2, 5, and 7, the cyclic separation processes were stable. Based on the profiles of NH_4^+ concentrations during the loading and washing steps (Figure 3b), the working capacity of the resin was restored for the cycles after the usage of fresh resin (first cycle), and there was practically no loss in the ammonium removal capacity. The NH_4^+ profiles during the regeneration and the second washing step (Figure 3c) were quite similar for the offline analyzed representative cycles (C1, C2, C5, and C7). It was a rather stable separation process in which the cation-exchange resin CS16GC was effectively regenerated by the 2 mol/L K_3PO_4 solution. The results were used to design the pilot-scale experiments for the same process.

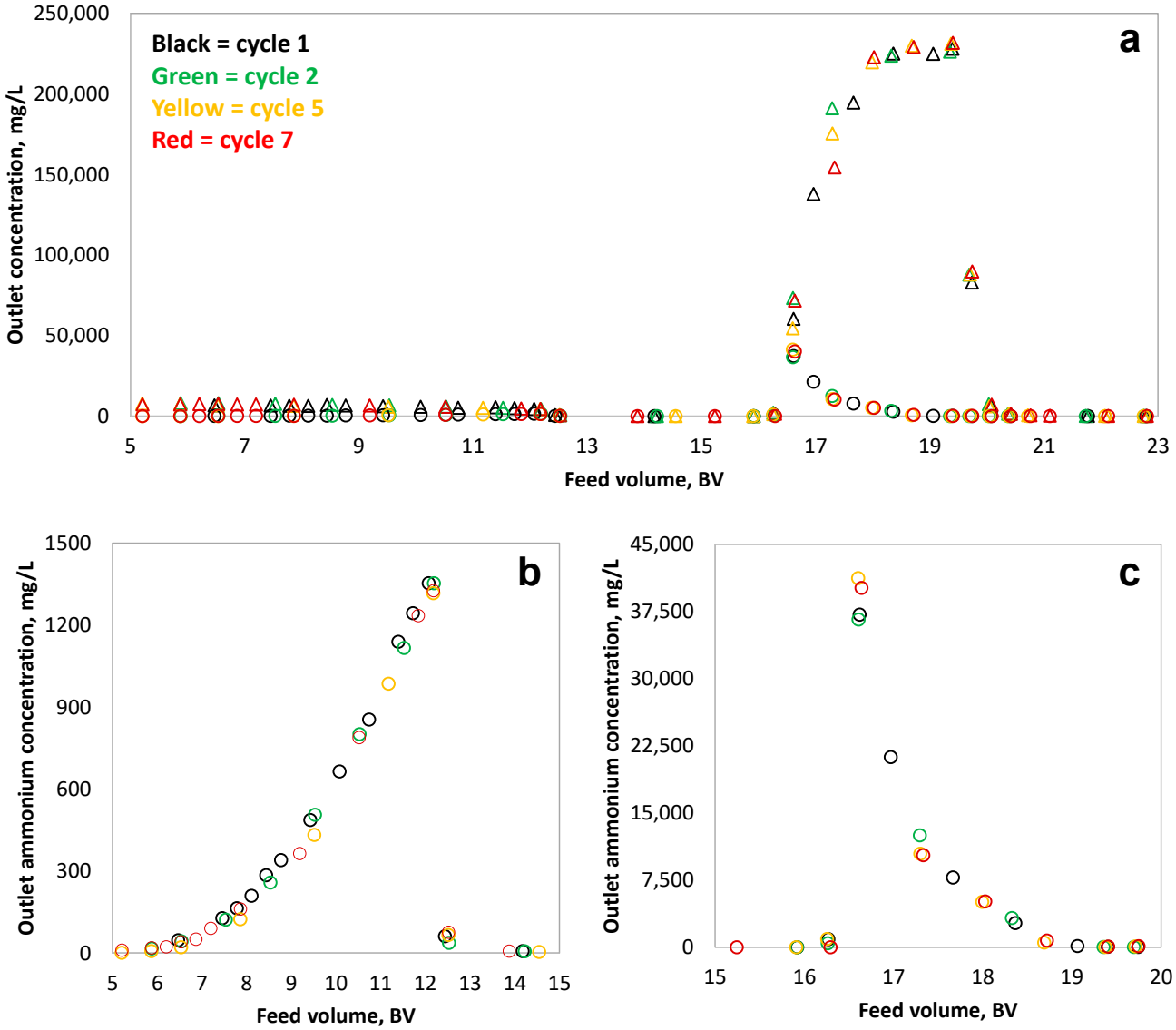

Figure 3. (**a**) Cyclic separation profiles of cycles 1, 2, 5, and 7 in laboratory-scale stability tests, (**b**) the ammonium profiles of loading, (**c**) the ammonium profiles of regeneration (CS16GC in K^+ form, V_{bed} = 35.34 mL, Q = 4 BV/h at 60 °C, loading: 12 BV 0.179 mol/L NH_4Ac, washing: 4 BV water, regeneration: 3 BV 2 mol/L K_3PO_4, second washing: 4 BV water). Triangles: K^+; circles: NH_4^+.

To determine the 'cut point' of the loading step in the pilot tests, the accumulated amount of NH_4^+ in the loading effluent was calculated based on the integration of NH_4^+

concentrations during the loading step of laboratory-scale test cycle 7 (Figure 4). According to the EU regulations regarding N emissions [34], the total N in the treated wastewater should be less than 10–15 mg/L. The loading volume 7 BV was chosen to result in a $NH_4^+ - N$ concentration of less than 10 mg/L in the loading step effluent. Moreover, at this point, the total removal efficiency was 99.76%, which was a good choice since the efficiency decreased at an accelerated rate after this point.

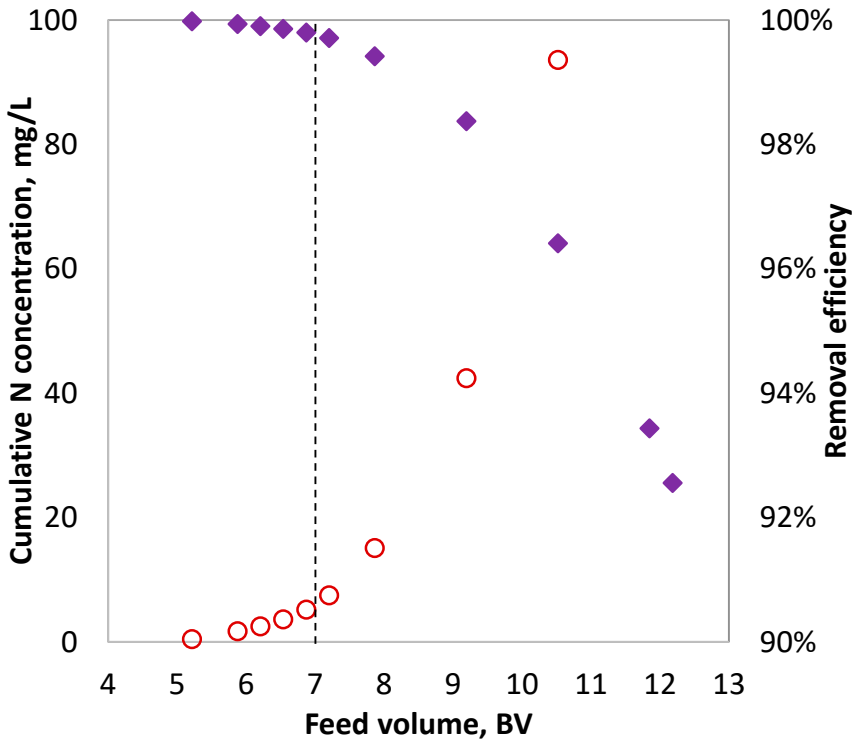

Figure 4. Ammonium removal during cycle 7 in laboratory-scale cyclic runs. Open circles: cumulative N concentration; solid diamonds: removal efficiency. CS16GC in K^+ form, V_{bed} = 35.34 mL, Q = 4 BV/h at 60 °C, loading: 12 BV 0.179 mol/L NH_4Ac, washing: 4 BV water, regeneration: 3 BV 2 mol/L K_3PO_4, second washing: 4 BV water.

3.4. Cyclic Separation on Pilot Scale

The pilot-scale tests were implemented for seven cycles with designed variations during cycles P3 and P4, which refer to the prolonged regeneration step (from normally 3 BV to 4 BV, shown as the green and yellow symbols in Figure 5a). In particular, during the first two cycles, there were disturbed column bed shaping and vast flow dispersion due to a gap (~1 cm) between the column head filter and the resin bed. The data for P2 in Figure 5 were based on a bed volume of 6.85 L (not 6.54 L as used in P3–P7) and, thus, not fully comparable to the later cycles.

The cumulative ammonium nitrogen concentrations in the effluent during the loading and washing steps are shown in Figure 5b. At the cut point of 7 BV, all the cycles generated purified water with a N content of less than 10 mg/L. If the first washing step was also included in the purified collection, the N concentration would exceed 10 mg/L in cycle 7 (P2 is not listed, as mentioned above). Generally, the goal of achieving a N content of less than 10 mg/L was achieved at the set cut point in the pilot-scale separation. The decision to collect the first washing step effluent depended on the actual requirements.

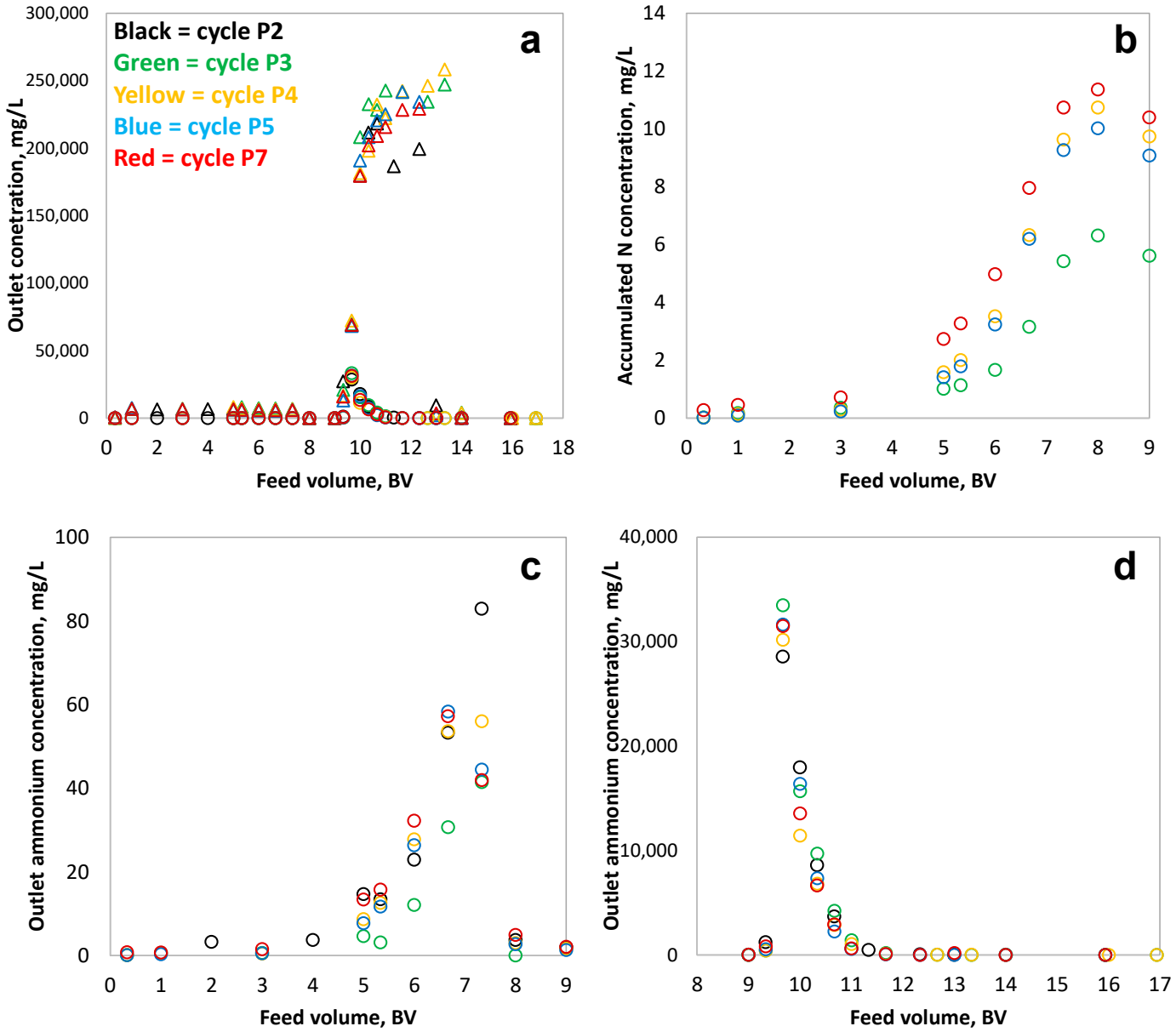

Figure 5. (**a**) Cyclic separation profiles of cycles 2, 3, 4, 5, and 7 in pilot-scale stability tests, (**b**) accumulated nitrogen concentration in the effluent, (**c**) the ammonium profiles of loading, (**d**) the ammonium profiles of regeneration (e.g., P2 = cycle 2 in pilot tests, CS16GC in K^+ form, V_{bed} = 6.54 L, Q = 4 BV/h at 60 °C. Details of loading, washing, and regeneration steps are given in Section 2.2.2 in the text.)). Triangles: K^+; circles: NH_4^+.

Using 2 mol/L K_3PO_4 for 3 BV cannot fully regenerate the resin bed, as shown in the regeneration study (Section 3.2). The negative effect of incomplete regeneration on the dynamic capacity of the column bed was enlarged in the pilot-scale experiment compared to that in the laboratory-scale tests. As revealed by the accumulated NH_4^+–N concentrations in the loading effluent (Figure 5b), the NH_4^+–N concentration in the collected effluent increased following the cycles, indicating a decreased NH_4^+ ion-exchange efficiency. It should be noted that, during regeneration with the 2 mol/L K_3PO_4 solution, ammonia gas came out of the effluent due to the highly basic condition. This issue can be solved by collecting the regeneration effluent in a closed system while neutralizing the basic solution. A pH adjustment is also a necessary measure to produce more applicable byproducts.

Figure 5c,d shows the NH_4^+ concentration profiles during the loading and washing steps and during the regeneration and second washing steps, respectively. The stability of

the pilot-scale separation process was not as good as that of the laboratory-scale separation process. However, the NH_4^+ profiles exhibited the same trend of forerunners. In particular, the profiles of cycles P4 and P5 were quite similar, with part of them overlapping each other (resulting in the same situation as in the N profiles of the loading effluent), indicating that one more BV of regeneration during cycles P3 and P4 benefitted the restoration of the uptake ability of the regenerated resin bed. That is, the resin bed was regenerated more thoroughly with a 4 BV of 2 mol/L K_3PO_4, which is consistent with the outcome of the regeneration study performed on the laboratory scale.

3.5. Regeneration Effluent as Liquid Compound Fertilizer

The regeneration agent K_3PO_4 was chosen over, for example, mineral acids because the aqueous phosphate could be reused as a fertilizer solution that contains N, K, and P elements. Such liquid compound fertilizers have a market value in household usage as nutrient suppliers for plants, such as those on lawns and flowers. As shown in Figure 6, the N/K ratio varied when the operating parameters (the concentration of K_3PO_4, with the volume being collected) were changed. In the laboratory regeneration experiments (Figure 6a), the resin beds were saturated with NH_4^+ before the regeneration efficiency tests. The N/K ratio approached 18.00 at the beginning of regeneration with 1 mol/L K_3PO_4, and the ratio range of 0.25–18.00 was obtained between 0.2 and 1.5 BV; for 2 mol/L K_3PO_4, the ratio was 0.10–3.36 between 0.2 and 1.5 BV. The concentrations of N and K during the regeneration are shown in Figure S4.

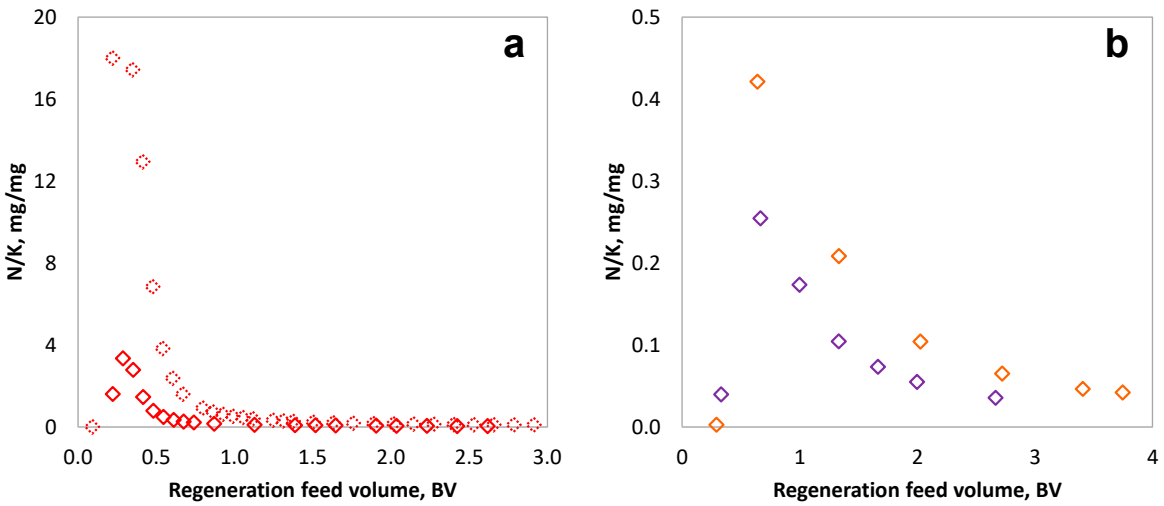

Figure 6. N/K ratio in the byproduct: (**a**) the data from regeneration experiments when 1 mol/L and 2 mol/L K_3PO_4 were both tested, (**b**) data based on 2 mol/L K_3PO_4 regeneration from laboratory cyclic tests cycle 7 with 12 BV loading and pilot experiments cycle P7 with 7 BV loading). Red symbols: regeneration tests; yellow symbols: laboratory test cycle 7; purple symbols: pilot test cycle 7. Dash-line symbols: 1 mol/L K_3PO_4; solid-line symbols: 2 mol/L K_3PO_4.

In the cyclic runs performed on the laboratory scale and pilot scale (Figure 6b), only 2 mol/L K_3PO_4 was applied as the regeneration agent, and the loading was cut at set points, which were before saturation. However, the N/K ratios in the byproduct were lower than in the pre-saturated situation. The byproduct N/K ratio of 0–0.42 resulted from C7 of the laboratory-scale cyclic runs, where loading was executed for 12 BV. However, the pilot-scale test data are relatively more realistic because the process parameters were set according to a real-world scenario with 7 BV loading. The N/K ratio varied in the range of 0.04–0.26 throughout the regeneration process, and the cut point for collecting the byproduct should reasonably be between 0.5 and 3 BV for a higher production rate. The concentrations of N and K during the regeneration in pilot-test cycle P7 are shown in Figure S5.

When requiring a higher N/K ratio, 1 mol/L K_3PO_4 should be used instead of 2 mol/L. According to the regeneration efficiency study (Section 3.2), more regeneration feeding of 1 mol/L K_3PO_4 is needed to fulfil the restoration of the resin bed. However, the predictable higher N/K ratio in the byproduct will take advantage of the agent exchange.

4. Conclusions

An industrial-level wastewater (condensate from a biomass treatment process) containing concentrated ammonium acetate (>3200 mg/L NH_4^+ and >8900 mg/L CH_3COO^-) was studied in ion-exchange processes for the recovery of NH_4^+. K_3PO_4 was used as the regeneration agent to generate a liquid compound fertilizer as a byproduct, which contains N, K, and P, elements that are required by plants. The N/K ratio in the byproduct was found to be adjustable by varying the concentration of the regeneration agent and the cut point of collecting the byproduct during the regeneration and second washing steps.

Two commercial cation ion-exchange resins, CS12GC and CS16GC, were compared based on their dynamic capacities towards NH_4^+ recovery. The CS16GC resin outperformed CS12GC due to its higher volumetric capacity. It was found that separation can be achieved at the same temperature (60 °C) at which the condensate is collected. This improves the energy efficiency of the overall process. It was found that 2 mol/L K_3PO_4 gave a higher regeneration efficiency (97.67% at 3 BV and ~100% at 4 BV), and it was thus used in the later experiments. In addition, it was proved that the presence of acetate in the feed does not prevent the use of a cation ion-exchange resin. The stability tests performed on a laboratory scale showed that the cyclic runs of the column separation process were steady and repeatable. The outcomes of the laboratory-scale tests were applied in the designation of the pilot-scale tests. A loading volume of 7 BV was set with a removal efficiency of 99.76% (according to the cycle 7 data from the cyclic laboratory runs), and regeneration was carried out with 2 mol/L K_3PO_4 for 3 (or 4) BV. The pilot column purified the feed and achieved the target NH_4^+ level in the treated effluent within the seven tested cycles, revealing that the industrial application of the cation ion-exchange resin CS16GC is worth further study. Additionally, although other cation ions, such as Na^+, K^+, Ca^{2+}, and Mg^{2+}, exist in trace amounts in real wastewater, they tend to occupy the active ion-exchange sites competing with NH_4^+, and it is harder to replace them with the concentrated K^+ in regeneration agents. Further studies on the effects of competitors and other impurities are suggested.

Supplementary Materials: The following supporting information can be downloaded at https://www.mdpi.com/article/10.3390/pr11030815/s1, Figure S1: Uptake of ammonium by CS12GC and CS16GC cation-exchange resins in K^+ form—the loading step; Figure S2. Acetate concentration at the outlet of the ion-exchange column during loading test; Figure S3: pH profile at the outlet of the ion-exchange column during loading test; Figure S4: Concentrations of accumulated N and K in the regeneration tests of CS16GC resin with K_3PO_4 on laboratory scale; Figure S5: Concentrations of accumulated N and K during the regeneration step of pilot cycle P7.

Author Contributions: Conceptualization, T.S. and J.H.; methodology, J.H., T.S. and J.S.; software, J.H. and T.S.; validation, J.S. and T.S.; formal analysis, J.S., J.H. and T.S.; investigation, J.S.; resources, T.S.; data curation, J.S. and T.S.; writing—original draft preparation, J.S.; writing—review and editing, J.S., T.S. and J.H.; visualization, J.S.; supervision, T.S. and J.H.; project administration, T.S.; funding acquisition, T.S. All authors have read and agreed to the published version of the manuscript.

Funding: This research was funded by the NITRO project co-financed by the Academy of Finland, decision number 315051, and LUT University. J.S. acknowledges a personal grant (decision number 45133) from Maaja Vesitekniikan Tukiry (MVTT) (Finland).

Data Availability Statement: The data presented in this study are available on request from the corresponding author.

Acknowledgments: The authors thank Petteri Peltola from Endev Oy for background information and useful discussions on the industrial applications of this research.

Conflicts of Interest: The authors declare no conflict of interest. The funders had no role in the design of the study; in the collection, analyses, or interpretation of the data; in the writing of the manuscript; or in the decision to publish the results.

References

1. Ye, Y.; Ngo, H.H.; Guo, W.; Liu, Y.; Chang, S.W.; Nguyen, D.D.; Liang, H.; Wang, J. A critical review on ammonium recovery from wastewater for sustainable wastewater management. *Bioresour. Technol.* **2018**, *268*, 749–758. [CrossRef]
2. Bernardi, M.; le Du, M.; Dodouche, I.; Descorme, C.; Deleris, S.; Blanchet, E.; Besson, M. Selective removal of the ammonium-nitrogen in ammonium acetate aqueous solutions by catalytic wet air oxidation over supported Pt catalysts. *Appl. Catal. B Environ.* **2012**, *128*, 64–71. [CrossRef]
3. Tekerlekopoulou, A.G.; Pavlou, S.; Vayenas, D.v. Removal of ammonium, iron and manganese from potable water in biofiltration units: A review. *J. Chem. Technol. Biotechnol.* **2013**, *88*, 751–773. [CrossRef]
4. Yan, T.; Ye, Y.; Ma, H.; Zhang, Y.; Guo, W.; Du, B.; Wei, Q.; Ngo, H.H. A critical review on membrane hybrid system for nutrient recovery from wastewater. *Chem. Eng. J.* **2018**, *348*, 143–156. [CrossRef]
5. EL-Bourawi, M.S.; Khayet, M.; Ma, R.; Ding, Z.; Li, Z.; Zhang, X. Application of vacuum membrane distillation for ammonia removal. *J. Membr. Sci.* **2007**, *301*, 200–209. [CrossRef]
6. Lubensky, J.; Ellersdorfer, M.; Stocker, K. Ammonium recovery from model solutions and sludge liquor with a combined ion exchange and air stripping process. *J. Water Process Eng.* **2019**, *32*, 100909. [CrossRef]
7. Cheng, W.P.; Chen, P.H.; Yu, R.F.; Ho, W.N. Treating ammonium-rich wastewater with sludge from water treatment plant to produce ammonium alum. *Sustain. Environ. Res.* **2016**, *26*, 63–69. [CrossRef]
8. Han, B.; Butterly, C.; Zhang, W.; He, J.Z.; Chen, D. Adsorbent materials for ammonium and ammonia removal: A review. *J. Clean. Prod.* **2021**, *283*, 124611. [CrossRef]
9. Iqbal, M.; Bhuiyan, H.; Mavinic, D.S. Assessing struvite precipitation in a pilot-scale fluidized bed crystallizer. *Environ. Technol.* **2008**, *29*, 1157–1167. [CrossRef]
10. Yigit, N.Ö.; Mazlum, S. Phosphate recovery potential from wastewater by chemical precipitation at batch conditions. *Environ. Technol.* **2007**, *28*, 83–93. [CrossRef]
11. Kumar Sinha, A.; Kumar Sasmal, A.; Pal, A.; Pal, D.; Pal, T. Ammonium phosphomolybdate $[(NH_4)_3PMo_{12}O_{40}]$ an inorganic ion exchanger for environmental application for purification of dye contaminant wastewater. *J. Photochem. Photobiol. A Chem.* **2021**, *418*, 113427. [CrossRef]
12. Joseph, J.; Radhakrishnan, R.C.; Johnson, J.K.; Joy, S.P.; Thomas, J. Ion-exchange mediated removal of cationic dye-stuffs from water using ammonium phosphomolybdate. *Mater. Chem. Phys.* **2020**, *242*, 122488. [CrossRef]
13. Thornton, A.; Pearce, P.; Parsons, S.A. Ammonium removal from digested sludge liquors using ion exchange. *Water Res.* **2007**, *41*, 433–439. [CrossRef]
14. Heinonen, J.; Sainio, T. Novel chromatographic process for the recovery and purification of hydroxy acids from alkaline spent pulping liquors. *Chem. Eng. Sci.* **2019**, *197*, 87–97. [CrossRef]
15. Heinonen, J.; Sainio, T. Modelling and performance evaluation of chromatographic monosaccharide recovery from concentrated acid lignocellulosic hydrolysates. *J. Chem. Technol. Biotechnol.* **2012**, *87*, 1676–1686. [CrossRef]
16. Sainio, T.; Turku, I.; Heinonen, J. Adsorptive removal of fermentation inhibitors from concentrated acid hydrolyzates of lignocellulosic biomass. *Bioresour. Technol.* **2011**, *102*, 6048–6057. [CrossRef] [PubMed]
17. DuPont Tech Fact. Ion Exchange Resins Selectivity. 2019. Available online: https://www.dupont.com/content/dam/dupont/amer/us/en/water-solutions/public/documents/en/IER-Selectivity-TechFact-45-D01458-en.pdf (accessed on 20 November 2022).
18. Gregor, H.P.; Bregman, J.I. Studies on ion-exchange resins. IV. Selectivity coefficients of various cation exchangers towards univalent cations. *J. Colloid Sci.* **1951**, *6*, 323–347. [CrossRef]
19. Chung, S.F.; Wen, C.Y. Longitudinal dispersion of liquid flowing through fixed and fluidized beds. *AIChE J.* **1968**, *14*, 857–866. [CrossRef]
20. Schiesser, W.E. *The Numerical Method of Lines: Integration of Partial Differential Equations*; Academic Press: San Diego, CA, USA, 1991.
21. Brown, P.N.; Byrne, G.D.; Hindmarsh, A.C. VODE: A Variable-Coefficient ODE Solver. *SIAM J. Sci. Stat. Comput.* **1989**, *10*, 1038–1051. [CrossRef]
22. Zhang, W.; Wang, Z.; Liu, Y.; Feng, J.; Han, J.; Yan, W. Effective removal of ammonium nitrogen using titanate adsorbent: Capacity evaluation focusing on cation exchange. *Sci. Total Environ.* **2021**, *771*, 144800. [CrossRef]
23. Harland, C.E. *Ion Exchange: Theory and Practice*; Royal society of Chemistry: London, UK, 1994.
24. Helfferich, F.G. *Ion Exchange*; Dover Publications: Mineola, NY, USA, 1995; Available online: https://books.google.fi/books?id=F9OQMEA88CAC (accessed on 20 November 2022).
25. Yoon, T.; Noh, B.; Moon, B. Parametric studies on the performance of cation exchange for the ammonium removal. *Korean J. Chem. Eng.* **2000**, *17*, 652–658. [CrossRef]
26. Gefeniene, A.; Kauspediene, D.; Snukiskis, J. Performance of sulphonic cation exchangers in the recovery of ammonium from basic and slight acidic solutions. *J. Hazard. Mater.* **2006**, *135*, 180–187. [CrossRef]
27. Wirthensohn, T.; Waeger, F.; Jelinek, L.; Fuchs, W. Ammonium removal from anaerobic digester effluent by ion exchange. *Water Sci. Technol.* **2009**, *60*, 201–210. [CrossRef]

28. Malovanyy, A.; Sakalova, H.; Yatchyshyn, Y.; Plaza, E.; Malovanyy, M. Concentration of ammonium from municipal wastewater using ion exchange process. *Desalination* **2013**, *329*, 93–102. [CrossRef]
29. Pinelli, D.; Foglia, A.; Fatone, F.; Papa, E.; Maggetti, C.; Bovina, S.; Frascari, D. Ammonium recovery from municipal wastewater by ion exchange: Development and application of a procedure for sorbent selection. *J. Environ. Chem. Eng.* **2022**, *10*, 108829. [CrossRef]
30. Truong, D.Q.; Loganathan, P.; Tran, L.M.; Vu, D.L.; Nguyen, T.V.; Vigneswaran, S.; Naidu, G. Removing ammonium from contaminated water using Purolite C100E: Batch, column, and household filter studies. *Environ. Sci. Pollut. Res.* **2022**, *29*, 16959–16972. [CrossRef]
31. Carocho, M.; Barreiro, M.F.; Morales, P.; Ferreira, I.C.F.R. Adding Molecules to Food, Pros and Cons: A Review on Synthetic and Natural Food Additives. *Compr. Rev. Food Sci. Food Saf.* **2014**, *13*, 377–399. [CrossRef]
32. Shi, X.; Akin, M.; Pan, T.; Fay, L.; Liu, Y.; Yang, Z. Deicer Impacts on Pavement Materials: Introduction and Recent Developments. *Open Civ. Eng. J.* **2009**, *3*, 16–27. [CrossRef]
33. Liu, Y.; Sheng, X.; Dong, Y.; Ma, Y. Removal of high-concentration phosphate by calcite: Effect of sulfate and pH. *Desalination* **2012**, *289*, 66–71. [CrossRef]
34. Preisner, M.; Neverova-Dziopak, E.; Kowalewski, Z. An Analytical Review of Different Approaches to Wastewater Discharge Standards with Particular Emphasis on Nutrients. *Environ. Manag.* **2020**, *66*, 694–708. [CrossRef]